Received June 2, 2017, accepted June 12, 2017, date of publication June 15, 2017, date of current version July 17, 2017.

Digital Object Identifier 10.1109/ACCESS.2017.2716103

Synchronous Motor-Generator Pair to Enhance Small Signal and Transient Stability of Power System With High Penetration of Renewable Energy

SIMING WEI, (Student Member, IEEE), YINGKUN ZHOU, (Student Member, IEEE), AND YONGZHANG HUANG, (Member, IEEE)

State Key Laboratory of Alternate Electrical Power System with Renewable Energy Sources, North China Electric Power University, Beijing 102206, China

Corresponding author: Siming Wei (siming_wei@ncepu.edu.cn)

This work was supported in part by the National Key Research and Development Program of China under Grant 2016YFB0101900 and in part by the Science and Technology Project of State Grid under Grant 5201011600TS.

ABSTRACT A synchronous generator is a key element in maintaining stability in the traditional power system and performs well. However, the high penetration of renewable energy will challenge the stable operation of the future power system, because the characteristics of converter-based resources differ from those of a synchronous generator. As a result, a weak grid caused by a lack of short circuit capacity and inertia, damping, and fault ride-through abilities become important issues for grid stability. To solve these problems, the synchronous motor-generator pair (MGP) was proposed as a possible approach. In this paper, first, state equations considering different frequencies on both sides of the MGP are established. The model for small signal stability is further modified to include the wind generator. On this basis, two systems are tested to investigate the performance of the MGP in small signal stability, torsional modes, rotor angle stability, and voltage support. Finally, on the basis of proposed control strategy, a closed-loop active power control of the MGP is realized by the 3-kW experimental system. The results show that the active power of the system is controllable. The MGP can provide sufficient inertia for frequency stability, restrain oscillation, and maintain rotor angle stability by higher damping and support the voltage.

INDEX TERMS High penetration of renewable energy, motor-generator pair (MGP), small signal stability, transient stability.

I. INTRODUCTION

It is a trend for the future power grid to be dominated by the increasing penetration of renewable energy [1], [2], bringing a fundamental change in grid structure and operation because the characteristics of converter-based resources are quite different from those of the traditional synchronous generator [3]–[7]. First, a power system with a large scale of renewable energy tends to be a weak grid [8]–[10]. ''Weak'' here has two meanings. One interpretation is that the converter cannot provide sufficient short circuit capacity and that the impedance of the AC system may be high, thus causing problems of reactive power and voltage instability [11]. The other meaning is low inertia. A synchronous generator can provide sufficient inertia to maintain frequency stability because of the synchronization relationship between its heavy rotor and grid frequency. However, the rotor speed of a wind generator is completely decoupled from grid frequency. Hence, the inertia response of a wind generator does not even exist, nor does solar photovoltaic [12], [13]. Inertia is also important for the satisfactory operation of high voltage DC transmission, which is known as the effective DC inertia constant [14], [15]. Second, renewable energy sources are increasingly vulnerable to large disturbances without the support of a synchronous generator. Converts cannot provide a high fault current and support overvoltage and low voltage during transient events, which seriously limits the fault ride-through capability of renewable energy sources [16], [17]. In addition, the complex dynamic interaction between renewable energy and power flow causes the uncertainty of damping, which is critical to restraining oscillation [18], [19].

Many solutions have been proposed to resolve the challenges mentioned above. A virtual synchronous generator mainly uses the energy stored in the rotor of a wind turbine or in an auxiliary energy storage unit to provide a sufficient inertia response [20]–[22]. The ''virtual'' means that the converter can mimic some characteristics of the synchronous generator by control. Similarly, the inertia control needs a sufficient reserve capacity to ensure that the generated active power can increase or decrease to respond to frequency deviation [23], [24]. The inertia energy can be from a wind turbine operating in the curtailing mode (5–10% of rated power) or an energy storage system. To damp oscillation, controllers are designed for the converter to produce a component of electromagnetic torque in phase with the rotor angle deviations [25]–[27]. Recently, a synchronous condenser was reused to improve grid stability not only for frequency response but also for short-circuit performance [10], [28].

Most of the existing solutions try to make the converter have some of the merits of a synchronous generator to maintain grid stability. However, it is not always easy for the converter to have satisfactory and reliable performance compared with a real synchronous machine, not only because of inherent disadvantages of the converter but also because of limitations such as fluctuation and cost.

Because the synchronous generator and synchronization are significant for grid stability, the necessity of replacing the traditional generator and how to reuse traditional generator to serve the future power system are worth discussing. Hence, we proposed the synchronous motor-generator pair (MGP) system for renewable energy integration [29], [30]. A simple single machine infinite bus system and open-loop experiments were tested [29]. However, after using the MGP, the power grid with high penetration of renewable energy will become a multi-machine system. The problems of rotor angle stability, voltage support and sub-synchronous oscillation still exist. The MGP should have the ability to flexibly control the active power like thermal power unit. Hence, the single-machine testing system in the published paper is not enough and a closed-loop experiment is necessary. Moreover, the structure of the MGP is so special because it connects two different electrical systems. Hence, the proposed analytical models in [29] and [30] should be modified in two aspects. One is state equations considering different frequencies on both sides, mainly for analysis of the torsional natural frequency. The other is to establish a comprehensive model considering wind generator, which is more accurate to reflect the characteristics of the whole system. These are the main works this paper has done.

The organization of this paper is as follows. Section II introduces the proposed MGP system and the possible future grid configuration. In Section III, models of the MGP system connected to a wind generator are established for small signal stability analysis. For this special system that connects two electrical systems, the case of different frequencies on both sides is also discussed. In Section IV, a single-machine infinite bus system is tested to investigate some basic characteristics of the MGP by comparing it with a traditional thermal power unit, and the oscillation modes are analyzed. Then, a 4-machine 2-area system is tested when the wind farm is connected to the grid using different proportions of MGP. Small signal stability, transient rotor angle and voltage stability are calculated. In Section V, closed-loop active power control of the MGP is realized by the proposed control strategy. The rotor angle relationship of the MGP is also verified by the experiment. Section VI gives conclusions and summarizes the key findings of this paper.

II. SYNCHRONOUS MGP SYSTEM FOR RENEWABLE ENERGY INTEGRATION

The proposed MGP system is shown in Fig.1(a) [30]. It consists of two synchronous machines, one operating as a motor and the other as a generator. Shafts of the two machines are coupled. Hence, the two machines can rotate at the same speed. The power generated by renewable energy (here are wind turbines) is converged to drive the motor. The motor replaces a steam turbine or a hydroturbine as a primary mover of the generator, which is a main difference from the traditional power generation unit. The converters with different kinds of renewable energy remain the same, which means that there is no need to add a high-capacity converter to drive the MGP.

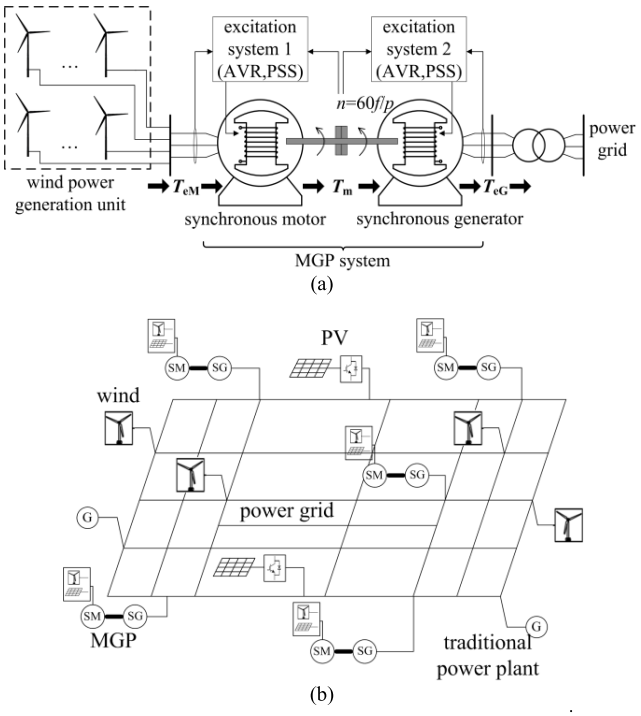

FIGURE 1. The proposed MGP system: (a) structure of MGP for wind farm integration; (b) a possible configuration of future power grid with MGP.

With the proposed MGP system, Fig.1(b) depicts a possible configuration of a future power grid with high penetration of renewable energy [29], [30]. One part of renewable energy is still connected to the grid in the traditional way, and another part can use the MGP for integration.

The moment of inertia is inherently provided by two synchronous machines. Damping and voltage control can be achieved by excitation systems. In this way, the MGP system can operate as a necessary complement to help future power grids dominated by converters enhance stability.

III. MODELING OF MGP SYSTEM FOR STABILITY ANALYSIS

A. STATE EQUATIONS BASED ON CLASSICAL MODEL OF SYNCHRONOUS MACHINE FOR SMALL SIGNAL STABILITY

In general, the motor and generator in an MGP system should have the same capacity, so the inertia constants are also the same. Hence, equations of motion of the two synchronous machines can be described as

$$\begin{cases} \dfrac{\mathrm{d}}{\mathrm{d}t}\Delta\omega_{\mathrm{M}} = \dfrac{1}{2H}(T_{\mathrm{eM}} - T_{\mathrm{m}} - K_{\mathrm{DM}}\Delta\omega_{\mathrm{M}}) \\ \dfrac{\mathrm{d}}{\mathrm{d}t}\delta_{\mathrm{M}} = \omega_0\Delta\omega_{\mathrm{M}} \end{cases} \tag{1}$$

$$\begin{cases} \dfrac{\mathrm{d}}{\mathrm{d}t}\Delta\omega_{\mathrm{G}} = \dfrac{1}{2H}(T_{\mathrm{m}} - T_{\mathrm{eG}} - K_{\mathrm{DG}}\Delta\omega_{\mathrm{G}}) \\ \dfrac{\mathrm{d}}{\mathrm{d}t}\delta_{\mathrm{G}} = \omega_0\Delta\omega_{\mathrm{G}} \end{cases} \tag{2}$$

where H is the inertia constant; T_{eM} and T_{eG} are electromagnetic torques of two machines; T_{m} is mechanical torque; δ_{M} and δ_{G} are rotor angles; ω_{M} and ω_{G} are rotor speeds; ω_0 is the base rotor electrical speed; K_{DM} and K_{DG} are damping coefficients.

In the analysis of the small signal stability, rotors of different machines are assumed to be made up of a single mass, which also means that $\omega_{\mathrm{M}} = \omega_{\mathrm{G}}$. Hence, the speed equations in (1) and (2) can be added directly.

$$\frac{\mathrm{d}}{\mathrm{d}t}\Delta\omega_r = \frac{1}{4H}[T_{\mathrm{eM}} - T_{\mathrm{eG}} - (K_{\mathrm{DM}} + K_{\mathrm{DG}})\Delta\omega_r] \tag{3}$$

To establish the rotor angle equation of the MGP, the rotor angle relationship of this special dual synchronous machine system should be investigated, as shown in Fig.2. E'_{M} and E'_{G} represent the internal voltages of motor and generator, and U_{M} and U_{G} are the terminal voltages. When ignoring the deviation of the rotor angle position, the relationship of two rotor angles can be expressed as

$$\delta_{\mathrm{M}} + \delta_{\mathrm{G}} = \delta_{\mathrm{MG}} \tag{4}$$

where δ_{MG} also equals the phase difference of bus voltages on both sides of the MGP if they are used as references to measure rotor angles.

For a traditional synchronous machine, the rotor angle changes with the output of active power. (4) shows that δ_{MG} has the same changing trend with δ_{M} and δ_{G}, which means it has the same changing trend with active power transmitted by the MGP, as shown in Fig.2. Hence, in this paper, δ_{MG} is considered an equivalent rotor angle of the MGP for modeling.

In addition, a power balance equation of the MGP system is needed (the air-gap torque is equal to the air-gap power in per unit)

$$T_{\mathrm{eM}} - T_{\mathrm{eG}} = p_{\mathrm{mloss}} \tag{5}$$

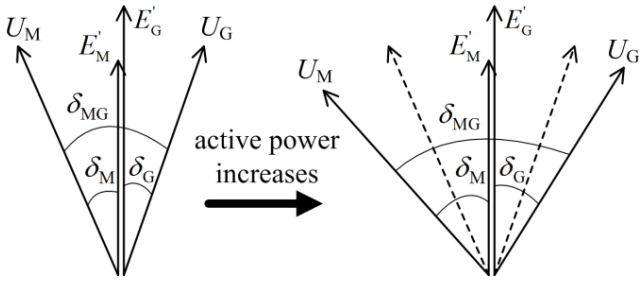

FIGURE 2. Rotor angle relationship of MGP.

where p_{mloss} is the mechanical loss per unit.

$$T_{\mathrm{eM}} = \frac{E'_{\mathrm{M}}U_{\mathrm{M}}}{X_{\sum 1}}\sin\delta_{\mathrm{M}}; \quad T_{\mathrm{eG}} = \frac{E'_{\mathrm{G}}U_{\mathrm{G}}}{X_{\sum 2}}\sin\delta_{\mathrm{G}}.$$

Assuming that p_{mloss} is constant when a small disturbance happens, (4) and (5) can be linearized.

$$\begin{cases} \Delta\delta_{\mathrm{M}} + \Delta\delta_{\mathrm{G}} = \Delta\delta_{\mathrm{MG}} \\ K_{\mathrm{sM}}\Delta\delta_{\mathrm{M}} - K_{\mathrm{sG}}\Delta\delta_{\mathrm{G}} = 0 \end{cases} \tag{6}$$

where K_{sM} and K_{sG} are synchronizing torque coefficients.

Hence, the deviation of the electromagnetic torque of the generator is

$$\Delta T_{\mathrm{eG}} = K_{\mathrm{sG}}\Delta\delta_{\mathrm{G}} = \frac{K_{\mathrm{sM}}K_{\mathrm{sG}}}{K_{\mathrm{sM}} + K_{\mathrm{sG}}}\Delta\delta_{\mathrm{MG}} \tag{7}$$

By substituting (6) and (7) into (2), state equations of MGP can be derived.

$$\frac{\mathrm{d}}{\mathrm{d}t}\begin{bmatrix}\Delta\omega_r \\ \Delta\delta_{\mathrm{MG}}\end{bmatrix} = \begin{bmatrix} \dfrac{-(K_{\mathrm{DM}} + K_{\mathrm{DG}})}{4H'} & \dfrac{-K_{\mathrm{sM}}K_{\mathrm{sG}}}{4H'(K_{\mathrm{sM}} + K_{\mathrm{sG}})} \\ \dfrac{K_{\mathrm{sM}} + K_{\mathrm{sG}}}{K_{\mathrm{sM}}}\omega_0 & 0 \end{bmatrix} \times \begin{bmatrix}\Delta\omega_r \\ \Delta\delta_{\mathrm{MG}}\end{bmatrix} + \begin{bmatrix}\dfrac{1}{4H'} \\ 0\end{bmatrix}\Delta T_{\mathrm{eM}} \tag{8}$$

B. STATE EQUATIONS CONSIDERING DIFFERENT ROTOR ELECTRICAL SPEEDS

Being different from traditional generation unit, the MGP system connects two electrical systems: one is a renewable power resource, and the other is a power grid. Hence, the frequencies on both sides are not always the same, which means that $\omega_{\mathrm{M}} \neq \omega_{\mathrm{G}}$. In this case, the MGP consists of two masses, as shown in Fig.3.

Hence, (1) and (2) can be rewritten as

$$\begin{cases} \dfrac{\mathrm{d}}{\mathrm{d}t}\Delta\omega_{\mathrm{M}} = \dfrac{1}{2H}[T_{\mathrm{eM}} - K(\delta_2 - \delta_1) - K_{\mathrm{DM}}\Delta\omega_{\mathrm{M}}] \\ \dfrac{\mathrm{d}}{\mathrm{d}t}\delta_{\mathrm{M}} = \omega_0\Delta\omega_{\mathrm{M}} \end{cases} \tag{9}$$

$$\begin{cases} \dfrac{\mathrm{d}}{\mathrm{d}t}\Delta\omega_{\mathrm{G}} = \dfrac{1}{2H}[K(\delta_2 - \delta_1) - T_{\mathrm{eG}} - K_{\mathrm{DG}}\Delta\omega_{\mathrm{G}}] \\ \dfrac{\mathrm{d}}{\mathrm{d}t}\delta_{\mathrm{G}} = \omega_0\Delta\omega_{\mathrm{G}} \end{cases} \tag{10}$$

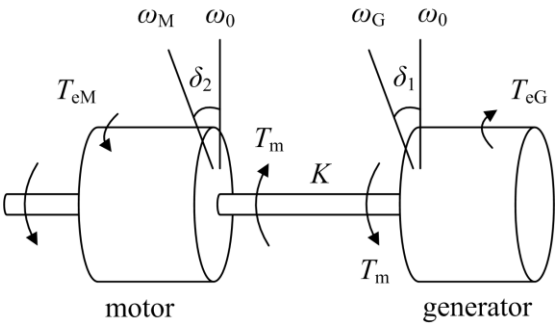

FIGURE 3. MGP represented by two masses.

where δ_1 and δ_2 represent the angular position of two machines and K is the shaft stiffness in p.u. torque/electrical rad.

By linearizing (9) and (10), the equations of rotor system of the MGP can be described as

$$\frac{\mathrm{d}}{\mathrm{d}t}\begin{bmatrix}\Delta\omega_G\\ \Delta\delta_G\\ \Delta\omega_M\\ \Delta\delta_M\end{bmatrix}=\begin{bmatrix}-\frac{K_{DG}}{2H} & -\frac{(K+K_{SG})}{2H} & 0 & \frac{K}{2H}\\ \omega_0 & 0 & 0 & 0\\ 0 & \frac{K}{2H} & -\frac{K_{DM}}{2H} & -\frac{K}{2H}\\ 0 & 0 & \omega_0 & 0\end{bmatrix}\times\begin{bmatrix}\Delta\omega_G\\ \Delta\delta_G\\ \Delta\omega_M\\ \Delta\delta_M\end{bmatrix}+\begin{bmatrix}0\\ 0\\ \frac{1}{2H}\\ 0\end{bmatrix}\Delta T_{eM} \quad (11)$$

C. STATE EQUATIONS OF THE MGP WITH A WIND GENERATOR

(8) shows that ΔT_{eM} of the MGP system is assumed to be zero when a small disturbance occurs. In a real system, the state variables of renewable energy sources should be added to the equations to comprehensively reflect the small signal characteristics of the MGP. In this paper, a double-fed induction generator (DFIG) is selected to illustrate modeling methods.

Obviously, the output power of a wind generator is equal to the input power of the motor in the MGP. Hence, the torque balance equation can be obtained.

$$T_{eDFIG} = T_{eM} \quad (12)$$

where T_{eDFIG} is the output torque of DFIG and can be expressed as

$$\Delta T_{eDFIG} = k_1\Delta E'_d + k_2\Delta E'_q + k_3\Delta i_{dr} + k_4\Delta i_{qr} \quad (13)$$

where E'_d and E'_q are components of the dq axis of the stator transient voltage; i_{dr} and i_{qr} are dq axis currents at the rotor side; $k_1 \sim k_4$ are coefficients related to parameters of DFIG.

Hence, the relationship between T_{eM} and the state variables of DFIG is established by (12) and (13).

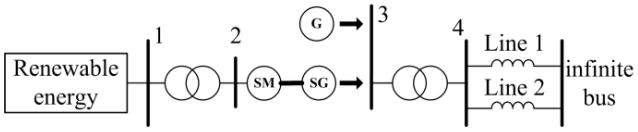

FIGURE 4. Single machine infinite bus test system.

Similarly, the currents also have a balance relationship

$$\begin{cases} i_{ds} + i_{dg} = i_{dM} \\ i_{qs} + i_{qg} = i_{qM} \end{cases} \quad (14)$$

where i_{ds} and i_{qs} are dq axis currents of DFIG at the stator side; i_{dg} and i_{qg} are dq axis currents on the grid side of the converter; and i_{dM} and i_{qM} are dq axis currents of the stator of the motor.

For the synchronous motor in the MGP, its linearized stator current can be expressed as

$$\begin{cases} \Delta i_{dM} = m_1\Delta\delta_M + m_2\Delta\psi_{fdM} \\ \Delta i_{qM} = n_1\Delta\delta_M + n_2\Delta\psi_{fdM} \end{cases} \quad (15)$$

where m_1, m_2, n_1, n_2 are coefficients related to the initial conditions and parameters of the machine, and ψ_{fdM} is the field flux linkage of the motor.

Hence, the relationship between the current of the motor and the current of the DFIG is established by (14) and (15). ψ_{fdM} in (15) means that the effects of the excitation dynamic are considered.

Based on the analysis above, the state equations of DFIG using the MGP for integration can be derived.

$$\frac{\mathrm{d}}{\mathrm{d}t}\begin{bmatrix}\mathbf{x}_{MGP}\\ \mathbf{x}_{DFIG}\end{bmatrix}=\begin{bmatrix}\mathbf{A}_{MGP} & \mathbf{A}_{12}\\ \mathbf{A}_{21} & \mathbf{A}_{DFIG}\end{bmatrix}\times\begin{bmatrix}\mathbf{x}_{MGP}\\ \mathbf{x}_{DFIG}\end{bmatrix} \quad (16)$$

where $\mathbf{x}_{MGP}$ and $\mathbf{x}_{DFIG}$ represent matrixes of state variables; $\mathbf{A}_{MGP}$ and $\mathbf{A}_{DFIG}$ are the original state matrixes; $\mathbf{A}_{12}$ and $\mathbf{A}_{21}$ are the new matrixes derived by (12)∼(15), which reflect the relationship between the DFIG and the MGP.

IV. CASE STUDY

A. COMPARISON OF MGP AND TRADITIONAL THERMAL POWER UNIT

In this part, a single machine infinite bus system is tested to analyze some basic characteristics of the MGP, as shown in Fig.4. A thermal power unit with the same capacity is selected for comparison. The parameters are listed in Table 1.

First, the small signal performance of the MGP is tested following a disturbance of loss of Line 1. Eigenvalues and damping ratios are shown in Table 2. The time response is then calculated by adding a rotor angle deviation of 5 degrees (0.087 rad), as shown in Fig.5.

Fig.5 shows that, on the one hand, the rate of change of the rotor angle deviation of the MGP is slightly higher, which means that the inertia of the MGP is lower than the inertia of the thermal power unit. However, this is sufficient for a power grid with a high penetration of renewable energy. On the other hand, the effect of MGP on damp oscillation is much better.

TABLE 1. Parameters of single machine infinite bus test system.

Parameters	Value
Rated active power (MW)	300
Rated voltage (kV)	20
Inertia constant (MW·s/MVA)	3.5
Damping coefficient (N·m·s/rad)	10
Transient reactance of machine (p.u.)	0.3
Reactance of transformer (p.u.)	0.15
Reactance of Line_1 (p.u.)	0.5
Reactance of Line_2 (p.u.)	0.93

TABLE 2. Calculation results of small signal stability.

Generation unit	Eigenvalue	Damping ratio
MGP	$-2.176 \pm j7.636$	0.274
Thermal power unit	$-0.714 \pm j6.347$	0.112

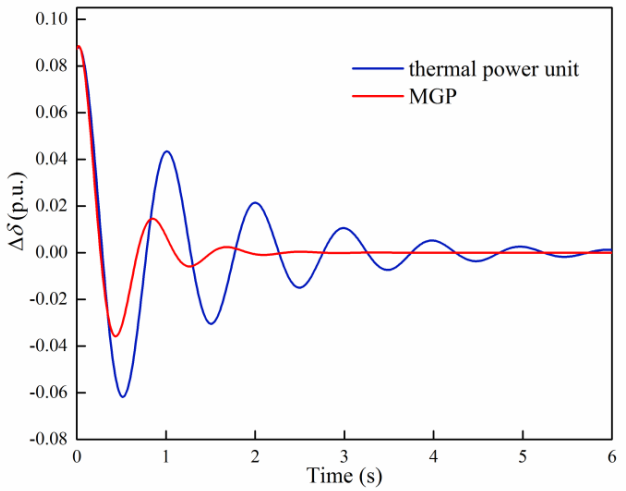

FIGURE 5. Time response of rotor angle.

The amplitude of the first swing and oscillation period are markedly improved. This damping effect can be explained by (3). MGP has two synchronous machines that provide two components of damping torque (K_{DM} and K_{DG}), which can significantly improve the damping level.

Then, the rotor angle stability of the MGP is tested following a three-phase fault on Line 1 when $t = 1$ s. The time response of the rotor angle is calculated with different fault-clearing times, as shown in Fig.6. In this case, the MGP and thermal power unit have the same initial rotor angles for comparison.

In Fig.6, both units can maintain rotor angle stability when the fault-clearing time is 1.060s. However, the MGP has a better dynamic process because of its higher damping. When the fault-clearing time is 1.089s, the thermal power unit shows a loss of synchronization, while the MGP still maintains stability. With the increasing fault-clearing time,

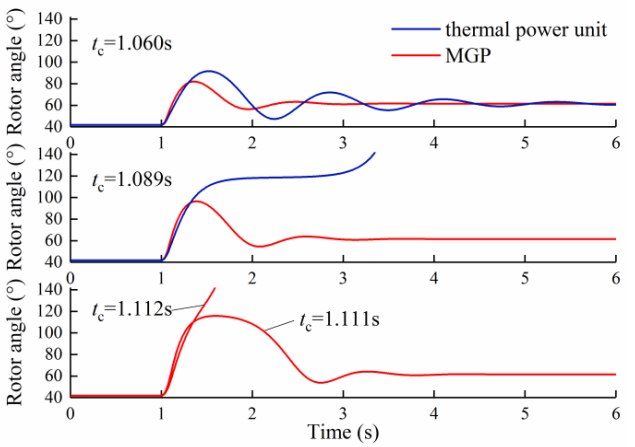

FIGURE 6. Rotor angle response with different fault-clearing times.

the MGP shows a loss of synchronization at 1.112s. The MGP has a longer critical fault-clearing time, a lower peak and a shorter oscillation period to maintain rotor angle stability.

Finally, the case of $\omega_M \neq \omega_G$ is calculated to analyze rotor natural frequencies and mode shapes of the MGP with different torsional stiffness, as shown in Fig.7.

In Fig.7(a), K is set to 70 p.u. torque/electrical rad. There are two oscillation modes. One mode is the 1.20Hz mode. This mode is also consistent with the result in Table 2, which represents the oscillation of the entire rotor against the power system. Two masses participate nearly equally in this mode. The other is the 24.16Hz mode with one polarity reversal, indicating that the rotor of the motor oscillates against the rotor of the generator when this mode is excited. With K increasing, the torsional natural frequency in this mode also increases, as shown in Fig.7(b).

B. COMPARISON OF WIND FARM INTEGRATION WITH AND WITHOUT THE MGP

In this part, a 4-machine 2-area system is tested to verify performance of the MGP when it is used for a wind farm. As shown in Fig. 8, the traditional generators connected to buses 2 and 4 are replaced by two wind farms with an output power of 1400MW. The wind generators are assumed to operate at maximum output mode. The total load of this grid is 2734MW; hence, the penetration rate is approximately 50%. In the wind farms, one part of the wind generators is connected to the grid in the traditional way, and another part converges to drive the MGP. The wind power transmitted by the MGP is set to 0% (wind farm integration without MGP), 20%, 60% and 100% by using different amounts of the MGP system. There are three testing scenarios.

1) SCENARIO 1 (SMALL SIGNAL STABILITY)

The calculation results for the small signal stability are shown in Table 3. Compared with the case of 0%, after using the MGP for grid-connection, the eigenvalue moves to the left of coordinate plane, and the damping ratio increases from 0.589 to 0.700. With the wind power transmitted by the MGP

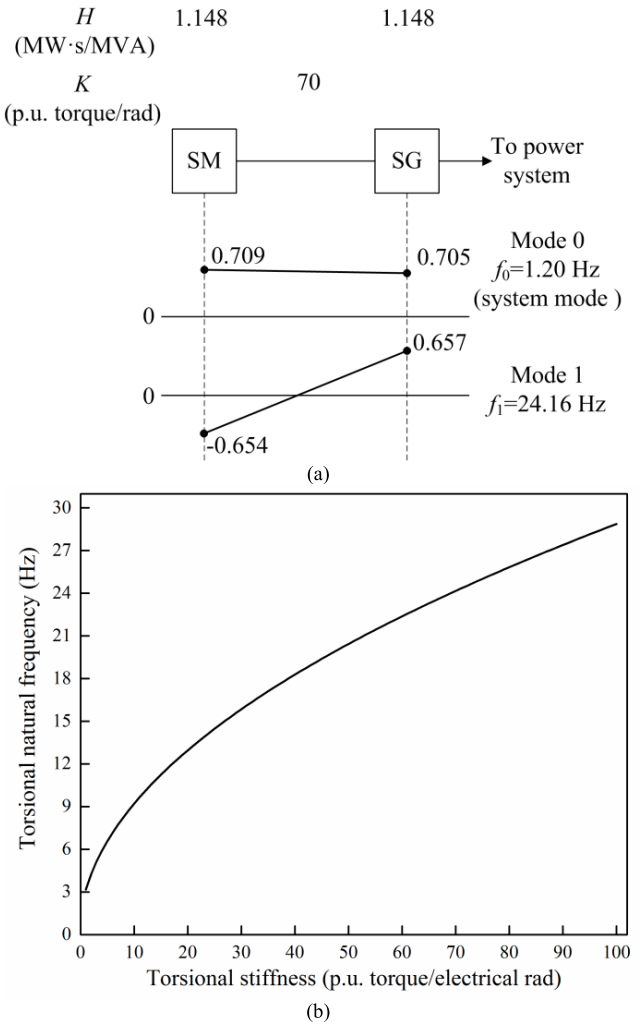

FIGURE 7. Rotor natural frequencies and mode shapes: (a) torsional nature frequency and mode shapes and (b) torsional nature frequency with different torsional stiffness.

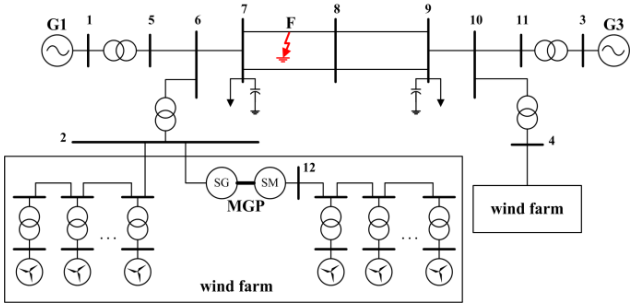

FIGURE 8. 4-machine 2-area test system.

increasing, the small signal stability is greatly improved, and the damping ratio finally reaches 0.894, which is more than 1.5 times that achieved in the case of 0%.

2) SCENARIO 2 (A TRANSIENT EVENT OF 200MW GENERATION LOSS)

In this scenario, the frequency immediately declines because of imbalance between load and generation. From Fig.9, with

TABLE 3. Calculation results of small signal stability.

Proportion of MGP(%)	Eigenvalue	Damping ratio
0	−0.739 ± j1.015	0.589
20	−1.090 ± j1.110	0.700
60	−1.169 ± j0.889	0.796
100	−1.126 ± j0.564	0.894

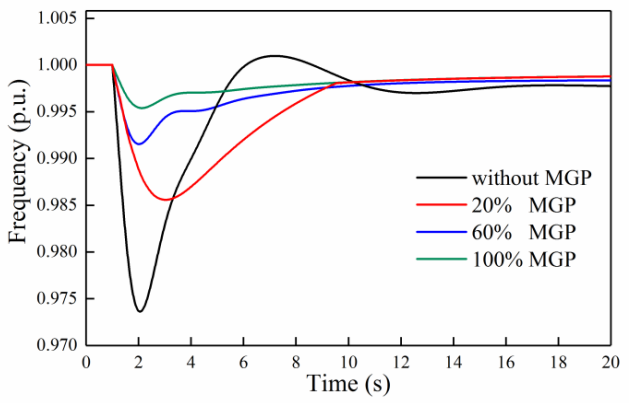

FIGURE 9. Frequency response with generation loss.

the proportion of the MGP increasing, the rate of change of frequency and the nadir are both improved. Compared with 0.974p.u. without the MGP, the frequency nadir is 0.995p.u. when all of the wind power uses the MGP for integration.

3) SCENARIO 3 (A THREE-PHASE FAULT OCCURS ON THE TRANSMISSION LINE AT POINT F)

In this scenario, the maximum rotor angle difference is used as an index to investigate rotor angle stability in different cases, as shown in Fig.10(a).

When the MGP is not used, the amplitude is high (the maximum rotor angle difference reaches 42.36°), and the period of oscillation is long. After using the MGP, with the proportion increasing, the maximum rotor angle difference is gradually dropping, and the oscillation is damped. When all of the wind generators use the MGP for integration, this value is 32.80°, which is a clear improvement. Fig.10(b) shows the voltage of bus 2, which is the point of common coupling (PCC) for wind farm integration. When the wind farm is connected to grid without the MGP, the voltage during fault has a large drop, which is controlled by voltage controller of converter. After using the MGP, the voltage level is significantly improved with the control of the excitation system.

V. EXPERIMENTS

The active power control strategy based on voltage phase difference between renewable energy source and the grid has been proposed and an open-loop experiment was done [29]. However, as a generation unit, the MGP must have the ability to control the output active power flexibly according to power order. This is also important for supporting stability.

The updated experimental system is shown in Fig.11(a) [30]. A closed-loop control strategy is designed

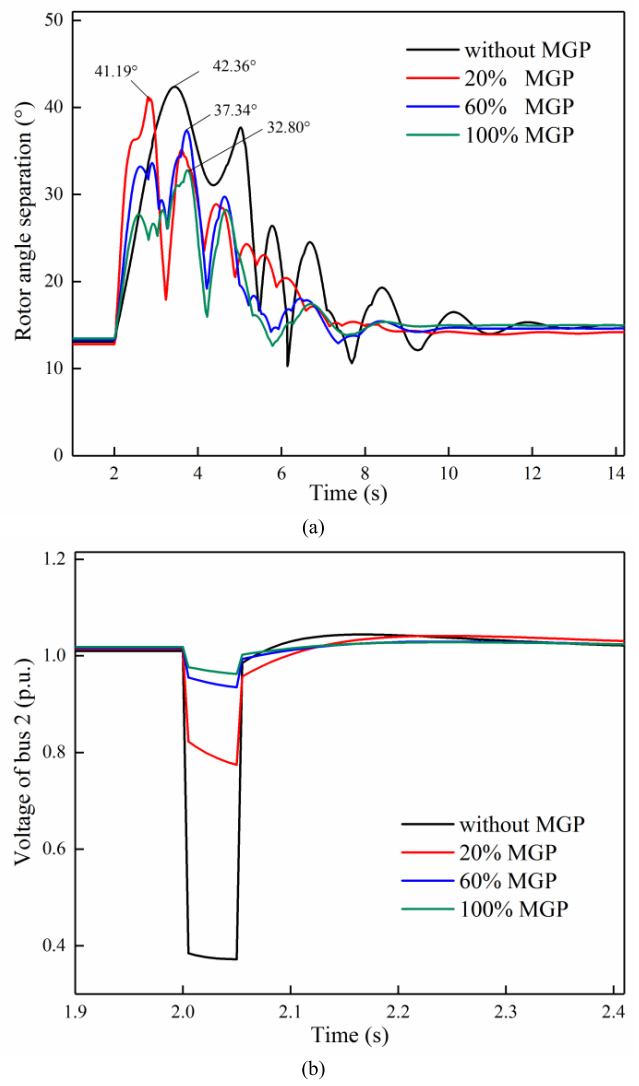

FIGURE 10. Rotor angle and voltage during fault: (a) rotor angle separation and (b) grid-connected voltage.

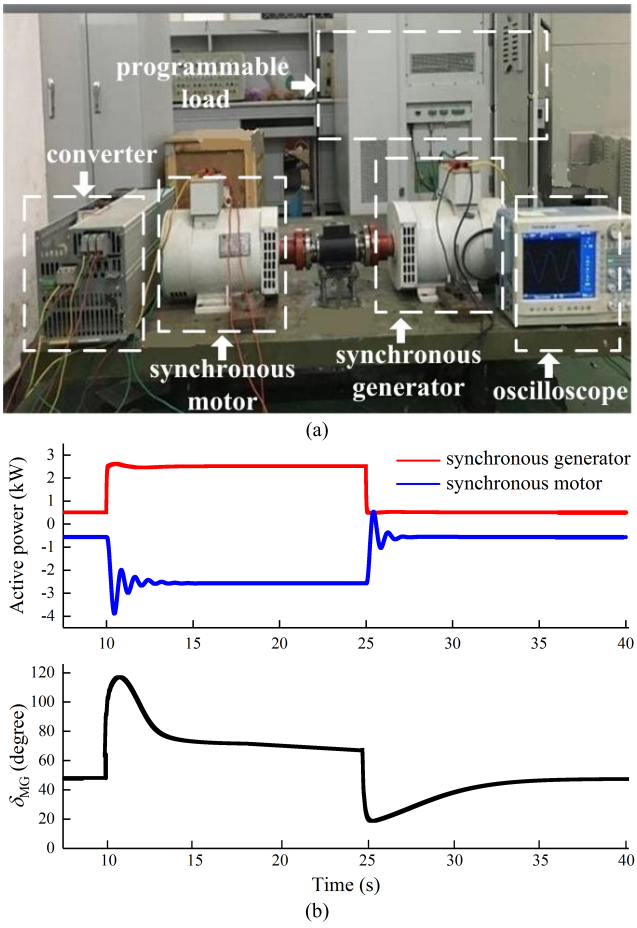

FIGURE 11. Experimental system and results. (a) 3kW MGP experimental system and (b) active power control and the equivalent rotor angle.

based on the proposed approach. In this experiment, the MGP is connected directly to the grid instead of the load. Hence, the voltage phase difference between renewable energy source and the grid is equal to the equivalent rotor angle (δ_{MG}).

Fig.11(b) shows that the MGP is stable in operation and the active power is 0.5kW before $t = 10$s. Then, the active power order is set to 2.5kW. The active power of both machines and δ_{MG} all increase and gradually reach to a new stable state. When $t = 25$s, the active power order changes from 2.5kW to 0.5kW. The active power transmitted by the MGP decrease. The δ_{MG} also drops. The experiment indicates that the active power of the MGP can be adjusted stably in a closed-loop control system and verifies the rotor angle relationship of the MGP described in Fig.2.

VI. CONCLUSION

The key contributions and findings of this paper are as follows:

1) The MGP can provide sufficient inertia for a power grid with high penetration of renewable energy. Two synchronous machines coupled by one shaft make it have reliable inertia response to maintain frequency stability.

2) The MGP has higher damping because two synchronous machines in the MGP system can provide two components of damping torque. As a result, the MGP can significantly damp oscillation and improve small signal stability.

3) In the analysis of torsional mode, the MGP can be regard as two masses. Hence, it has one torsional natural frequency. This can help to analyze the sub-synchronous oscillation.

4) The future power grid with MGP is actually a multi-machine system. The damping effects make it have a longer critical fault-clearing time, lower peak and shorter oscillation period, which also help maintain the transient rotor angle stability. The voltage stability during the transient events can be effectively improved by the synchronous generator. This is mainly achieved by the synchronous generator in the MGP.

5) The active power transmission of the MGP can be controlled by the proposed closed-loop control strategy. This is important for the MGP drived by converter of renewable energy to realize flexible power regulation like conventional power generation unit.

REFERENCES

[1] J. L. Sawin, K. Seyboth, and F. Sverrisson, "Renewables 2016: Global status report," Secretariat, Paris, France, Tech. Rep. REN21, 2016.
[2] H. Lund and B. V. Mathiesen, "Energy system analysis of 100% renewable energy systems—The case of Denmark in years 2030 and 2050," *Energy*, vol. 34, no. 5, pp. 524–531, May 2009.
[3] N. Miller, C. Loutan, M. Shao, and K. Clark, "Emergency response: US system frequency with high wind penetration," *IEEE Power Energy Mag.*, vol. 11, no. 6, pp. 63–71, Nov./Dec. 2013.
[4] N. W. Miller, "Keeping it together: Transient stability in a world of wind and solar generation," *IEEE Power Energy Mag.*, vol. 13, no. 6, pp. 31–39, Nov./Dec. 2015.
[5] K. G. Boroojeni, M. H. Amini, and S. S. Iyengar, "Overview of the security and privacy issues in smart grids," in *Smart Grids: Security and Privacy Issues*. New York, NY, USA: Springer, 2017, pp. 1–16.
[6] J. Conto, "Grid challenges on high penetration levels of wind power," in *Proc. IEEE Power Energy Soc. Gen. Meet.*, San Diego, CA, USA, Jul. 2012, pp. 1–3.
[7] D. P. Kothari and I. J. Nagrath, *Modern Power System Analysis*, 3rd ed. New York, NY, USA: McGraw-Hill, 2006.
[8] Y. Zhang, S. F. Huang, J. Schmall, J. Conto, J. Billo, and E. Rehman, "Evaluating system strength for large-scale wind plant integration," in *Proc. IEEE PES Gen. Meet. Conf. Expo.*, Jul. 2014, pp. 1–5.
[9] J. W. Feltes and B. S. Fernandes, "Wind turbine generator dynamic performance with weak transmission grids," in *Proc. IEEE Power Energy Soc. Gen. Meet.*, San Diego, CA, USA, Sep. 2012, pp. 1–7.
[10] N. A. Masood, R. Yan, T. K. Saha, and S. Bartlett, "Post-retirement utilisation of synchronous generators to enhance security performances in a wind dominated power system," *IET Gener. Transm. Distrib.*, vol. 10, no. 13, pp. 3314–3321, Oct. 2016.
[11] S. H. Huang, J. Schmall, J. Conto, J. Adams, Y. Zhang, and C. Carter, "Voltage control challenges on weak grids with high penetration of wind generation: ERCOT experience," in *Proc. IEEE Power Energy Soc. Gen. Meet.*, San Diego, CA, USA, Jul. 2012, pp. 1–7.
[12] H. Golpîra, H. Seifi, A. R. Messina, and M. Haghifam, "Maximum penetration level of micro-grids in large-scale power systems: Frequency stability viewpoint," *IEEE Trans. Power Syst.*, vol. 31, no. 6, pp. 5163–5171, Mar. 2016.
[13] Y. Wang, V. Silva, and M. Lopez-Botet-Zulueta, "Impact of high penetration of variable renewable generation on frequency dynamics in the continental Europe interconnected system," *IET Renew. Power Gener.*, vol. 10, no. 1, pp. 10–16, Jan. 2016.
[14] *IEEE Guide for Planning DC Links Terminating at AC Locations Having Low Short-Circuit Capacities, Part I: AC/DC System Interaction Phenomena*, IEEE Standard 1204-1997, 1997. [Online]. Available: http://ieeexplore.ieee.org/document/653230/
[15] P. Kundur, *Power System Stability and Control*. New York, NY, USA: McGraw-Hill, 1994.
[16] S. Alyami, Y. Wang, C. Wang, J. Zhao, and B. Zhao, "Adaptive real power capping method for fair overvoltage regulation of distribution networks with high penetration of PV systems," *IEEE Trans. Smart Grid*, vol. 5, no. 6, pp. 2729–2738, Nov. 2014.
[17] H. Ahmadi, A. Ellis, and J. R. Marti, "Voltage management challenges in feeders with high penetration of distributed generation," in *Proc. IEEE CCECE*, Vancouver, BC, Canada, May 2016, pp. 1–6.
[18] X. Zhang, C. Lu, S. Liu, and X. Wang, "A review on wide-area damping control to restrain inter-area low frequency oscillation for large-scale power systems with increasing renewable generation," *Renew. Sustain. Energy Rev.*, vol. 57, pp. 45–58, May 2016.
[19] R. H. Byrne *et al.*, "Small signal stability of the western North American power grid with high penetrations of renewable generation," in *Proc. IEEE Photovolt. Specialists Conf. (PVSC)*, Portland, OR, USA, Jun. 2016, pp. 1784–1789.
[20] H. P. Beck and R. Hesse, "Virtual synchronous machine," in *Proc. IEEE EPQU Conf.*, Barcelona, Spain, Sep. 2007, pp. 1–6.
[21] K. Visscher and S. W. H. De Haan, "Virtual synchronous machines (VSG's) for frequency stabilisation in future grids with a significant share of decentralized generation," in *Proc. CIRED*, 2008, pp. 1–4.
[22] Q. C. Zhong and G. Weiss, "Synchronverters: Inverters that mimic synchronous generators," *IEEE Trans. Ind. Electron.*, vol. 58, no. 4, pp. 1259–1267, Apr. 2011.
[23] M. Reidy, H. Mokhlis, and S. Mekhilef, "Inertia response and frequency control techniques for renewable energy sources: A review," *Renew. Sustain. Energy Rev.*, vol. 69, pp. 144–155, Nov. 2017.
[24] A. B. T. Attya and T. Hartkopf, "Utilising stored wind energy by hydro-pumped storage to provide frequency support at high levels of wind energy penetration," *IET Gener. Transm. Distrib.*, vol. 9, no. 12, pp. 1485–1497, Apr. 2015.
[25] R. Yousefian, R. Bhattarai, and S. Kamalasdan, "Transient stability enhancement of power grid with integrated wide-area control of wind farms and synchronous generators," *IEEE Trans. Power Syst.*, to be published. [Online]. Available: http://ieeexplore.ieee.org/document/7867871/
[26] J. L. Domínguez-García, O. Gomis-Bellmunt, and F. D. Bianchi, "Power oscillation damping supported by wind power: A review," *Renew. Sustain. Energy Rev.*, vol. 16, no. 7, pp. 4994–5006, Sep. 2012.
[27] H. Geng, X. Xi, L. Liu, G. Yang, and J. Ma, "Hybrid modulated active damping control for DFIG based wind farm participating in frequency response," *IEEE Trans. Energy Convers.*, to be published. [Online]. Available: http://ieeexplore.ieee.org/abstract/document/7850989/
[28] R. Yan, T. K. Saha, and N. Modi, "Frequency response and its enhancement using synchronous condensers in presence of high wind penetration," in *Proc. IEEE Power Energy Soc. Gen. Meet.*, Denver, CO, USA, Jul. 2016, pp. 1–5.
[29] S. Wei, Y. Zhou, S. Li, and Y. Huang, "A possible configuration with motor-generator pair for renewable energy integration," *CSEE J. Power Energy Syst.*, vol. 3, no. 1, pp. 93–100, 2017.
[30] S. Wei, Y. Zhou, G. Xu, and Y. Huang, "Motor-generator pair: A novel solution to provide inertia and damping for power system with high penetration of renewable energy," *IET Gener. Transm. Distrib.*, vol. 11, no. 7, pp. 1839–1847, 2017.

SIMING WEI (S'16) received the M.S. degree from North China Electric Power University, Beijing, China, in 2015, where he is currently pursuing the Ph.D. degree. His research interests include stability of renewable energy power system and power electronics.

YINGKUN ZHOU (S'16) received the M.S. degree from North China Electric Power University, Beijing, China, in 2015, where he is currently pursuing the Ph.D. degree. His research interests include stability of renewable energy power system and power electronics.

YONGZHANG HUANG (M'14) received the B.S. degree from the Department of Engineering Physics, Tsinghua University, Beijing, China, in 1984, and the Ph.D. degree in physics from the Chinese Academy of Sciences in 1991. He is currently a Professor with the Department of Electrical Engineering, North China Electric Power University, Beijing. He is also a Chinese Distinguished Expert of the Thousand Talents Program and the Deputy Director of the State Key Laboratory of the Renewable Energy Power System. His current research interests include renewable energy power systems, high power electronic devices and applications, electric vehicles, and big data of the power grid.